

DNA engineering and its application to nanotechnology

Nadrian C. Seeman

The combination of branched DNA molecules and 'sticky' ends creates a powerful molecular assembly kit for structural DNA nanotechnology. Polyhedra, complex topological objects, a nanomechanical device and two-dimensional arrays with programmable surface features have already been produced in this way. Future applications range from macromolecular crystallography and new materials to molecular electronics and DNA-based computation.

What is DNA engineering? Many biotechnologists design sequences in the hope of improving the performance of DNA in a cellular context, either to modify the level of gene expression or to optimize the nature of gene products; likewise, the antisense enterprise is often concerned with modifying the molecular features of natural DNA. However, our interest here lies in neither of these activities. For the purpose of this article, DNA engineering consists of selecting sequences of DNA molecules with conventional nucleotides, for the nanotechnological purpose of creating specific topologies, shapes and arrangements of secondary and tertiary structure.

We are all aware that the key to DNA's biological role lies in the specificity of the base pairing that holds the two strands of the double helix together: adenine (A) pairs with thymine (T) and guanine (G) pairs with cytosine (C). The familiar double helix that results from these complementary interactions is a linear molecule, in the topological sense that its axis is not branched. However, by designing appropriate sequences, it is possible in synthetic systems to produce branched DNA molecules¹ (Fig. 1a). This molecule is an analog of a biologically important branched DNA molecule: the Holliday junction², from which it is derived, is an intermediate in genetic recombination. However, the naturally occurring Holliday junction is usually formed between two duplex molecules with the same sequence. This sequence symmetry destabilizes the position of the branch point so that it is free to migrate. Selecting sequences that eliminate this symmetry leads to branched molecules, termed 'junctions', whose branch points are fixed¹. It is evident that the addition of 'sticky' ends to branched molecules produces components that can lead to association and ligation products more complex than would be obtained from linear DNA, including stick polyhedra, knots and catenanes, devices and networks (Fig. 1b). A DNA double helix is about 2 nm wide and its helical repeat is 10–10.6 bp, which produces a pitch of 3.4–3.6 nm. Thus, constructions made from DNA will have features on the nanometer scale.

Why would anyone wish to produce such target species? There are several practical ends to which we

N. C. Seeman (ned.seeman@nyu.edu) is at the Department of Chemistry, New York University, New York, NY 10003, USA.

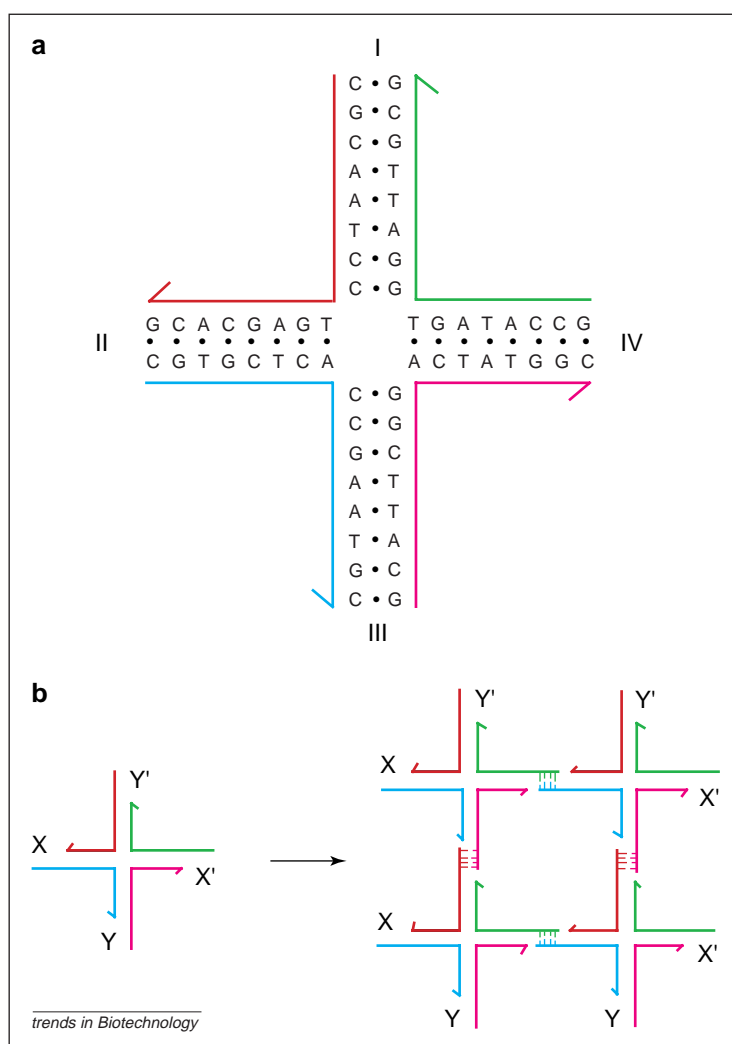


Figure 1

(a) A branched DNA molecule with four arms. The four strands, here identified by color, combine to produce four arms, labeled with Roman numerals. The branch point of this molecule is fixed. (b) The formation of a two-dimensional lattice from a four-arm junction with sticky ends. X and Y are sticky ends, and X' and Y' are their complements. Four of the monomeric junctions on the left are complexed in parallel orientation to yield the structure on the right. DNA ligase can close the gaps left in the complex. The complex has maintained open valences, so that it could be extended by the addition of more monomers. A DNA double helix is about 200 nm wide and its helical repeat is 10–10.6 bp, which produces a pitch of 340–360 nm. Thus, constructions made from DNA will have features on the nanometer scale.

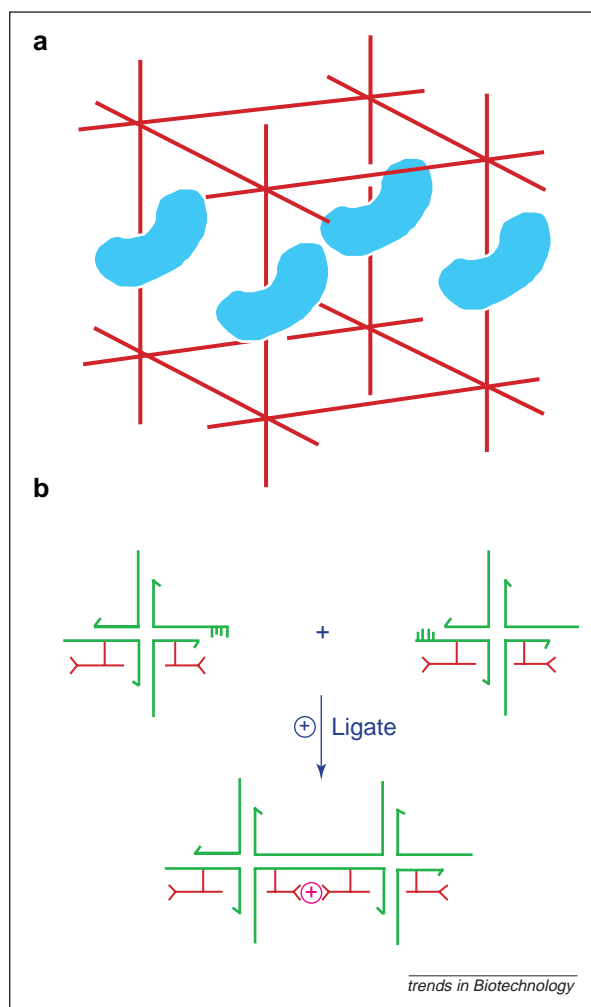


Figure 2

Future applications of DNA nanotechnology. **(a)** The DNA lattice, drawn in red, forms a simple cubic lattice made from six-armed junctions. The blue kidney-bean-shaped features show the potential for including 'guest' molecules in each unit cell. If the guests can be aligned parallel to each other, their structures can be determined by X-ray crystallography. **(b)** Two branched junctions are shown in green with a red molecular wire attached to them. When the two junctions stick to each other, so does the molecular wire, which forms a synapse-like structure. This drawing represents one way that branched DNA could be used as a scaffold to organize molecules whose properties are best suited to a particular molecular task.

expect these molecules can be applied. First, spatially periodic networks are crystals. The ability to build stick-figure crystalline cages on the nanometer scale could be used to orient other molecules as 'guests' inside those cages, thereby rendering their structures amenable to diffraction analysis (Fig. 2a). Second, the same types of crystalline array could be used to position and orient components of molecular-electronic devices with nanometer-scale precision (Fig. 2b). Third, nanomechanical devices can lead to nanometer-scale robotics. Fourth, DNA nanotechnology can create motifs that are useful for DNA-based computation and the algorithmic assembly of materials³.

Given goals of this nature, one must ask the reverse question: why use DNA to achieve them? First, DNA sticky ends provide the most predictable, diverse, reliable

and programmable set of intermolecular interactions available. In contrast to other molecules on their size scale (e.g. proteins), it is very simple to program associations between specific molecules through complementarity. It is important to realize that sticky ends provide not only predictable affinity⁴ but also predictable local product structure: they associate to form B-DNA⁵. The relative orientations of the associating molecules are known with greater precision than the associations of other systems used for crystal engineering⁶.

Second, convenient automated phosphoramidite chemistry⁷ permits the assembly of arbitrary sequences containing more than a hundred nucleotides. The needs of the biotechnology industry have resulted in numerous modified phosphoramidites that can be used for special purposes. Third, DNA molecules can be manipulated by commercially available enzymes – they can be joined by DNA ligases, cleaved at specific sites by restriction enzymes, phosphorylated by kinases and have their topology altered by DNA topoisomerases. Cyclic targets can be readily purified from linear failure products by treatment with exonucleases. Fourth, DNA contains an externally readable code⁸ that ultimately may be used to position and orient scaffolded molecules.

Third, DNA is a stiff polymer. Electron micrographs of DNA have often led us to think of DNA as a spaghetti-like molecule. However, those pictures are of very long molecules, containing hundreds of persistence lengths (a measure of the contour length over which segments of a rod-like object are correlated). The persistence length of DNA is about 500 Å under conventional conditions⁹ and the lengths in which we are interested are only 70–100 Å long (two to three turns). For comparison, the persistence length of spaghetti is about 1.5 cm and so, if we were working with spaghetti, we would be thinking of lengths of only 2–3 mm, over which it does not bend very much.

Sequence selection

The branch points of Holliday junctions are flanked by two symmetrical sequences; eliminating this symmetry fixes the branch-point's location. In addition, the design of junction sequences entails the elimination of sequence symmetry between contiguous nucleotide groups: sequences are divided into a series of overlapping 4–6 nucleotide elements, and repeated elements are forbidden during the sequence-selection process; likewise, the complements to all elements flanking branch points are also avoided¹. This simple approach aims to eliminate all possible alternative structures that the system could assume; it has proved to be remarkably successful in the design of DNA molecules containing branch points^{10,11}. A lot of effort is devoted to the sequence-selection process, because branched target molecules correspond to an excited state and care must be taken to ensure that the excited product obtained is the one that is sought.

Branch flexibility

The assembly of the quadrilateral product shown in Fig. 1b assumes not only that the sticky ends associate in a specific fashion but also that the junctions maintain fixed angles between their double-helical arms. Unfortunately, this assumption is not correct. Individual

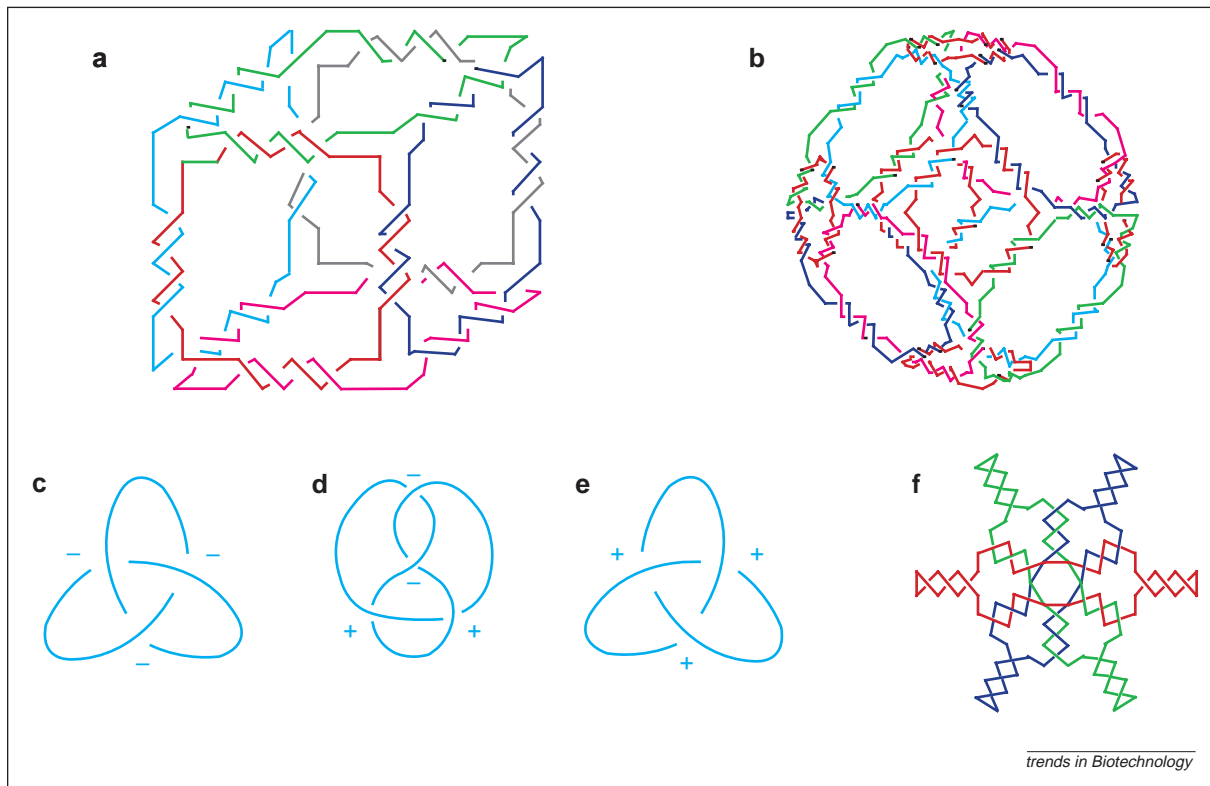


Figure 3

Ligated products from flexible DNA components. **(a)** A cube and **(b)** a truncated octahedron with their edges formed by two turns of double-helical DNA. The twisting is confined to the central portion of each edge for clarity but actually extends from vertex to vertex. Both molecules are drawn as though they were constructed from three-armed junctions, but the truncated octahedron has been constructed from four-armed junctions, which has been omitted for clarity. **(c–e)** Knots constructed from DNA: **(c)** a trefoil knot with negative nodes; **(d)** a figure-of-eight knot; **(e)** a trefoil knot with positive nodes. The signs of the nodes are indicated. **(f)** Borromean rings: scission of any of the three rings (red, blue or green) results in the unlinking of the other two rings.

junctions have flexible angles around their branch points^{12,13}; we will see below that this problem can be solved by using multiple junctions as building blocks. However, control over the ligation products of single junctions is restricted to the topological level and, similarly, proof of synthesis is only topological and not geometrical. A series of junctions with a unique set of sticky ends can be joined to form discrete low-symmetry closed products but rigid subunits are necessary to form high-symmetry targets, such as periodic arrays.

Nanoscale products from flexible junctions

Flexible building blocks have been used to construct a variety of topological targets. The first of these (Fig. 3a) was a DNA molecule whose helix axes are connected like the edges of a cube or a rhombohedron¹⁴. Each edge contains two turns of double-helical DNA and, as a consequence of this design, each face corresponds to a cyclic single strand. Each of these strands is linked twice to each of its neighbors, resulting in a complex hexacatenane. The topology has been demonstrated by designing a unique restriction site in each edge and then digesting the product at those sites to yield the predicted subcatenanes¹⁴. A more complex DNA molecule with the connectivity of a truncated octahedron¹⁵ was built by a solid-support-based method¹⁶ (Fig. 3b). This contains 14 faces, six squares and eight hexagons. As with the cube, each edge contains

two turns of DNA and so this molecule is a complex 14-catenane. The topology has been demonstrated by techniques similar to those used above.

The half turn of DNA corresponds to the fundamental unit of braiding topology: the node, or a crossing seen when a topological figure is projected in two dimensions¹⁷. This feature makes branched DNA a particularly useful component with which to build complex topological figures. This property has allowed the construction of a trefoil knot with negative nodes (Fig. 3c) from a three-armed branched junction with a single half turn in each arm¹⁸. By combining right-handed B-DNA with left-handed Z-DNA, a figure-of-eight knot has also been assembled¹⁹ (Fig. 3d), as has a trefoil knot with positive nodes, by using Z-DNA exclusively²⁰ (Fig. 3e). These latter knots have entailed the use of unusual DNA motifs but they have not been simple branches. An RNA knot built this way has been used to demonstrate that *Escherichia coli* DNA-topoisomerase III has an RNA-topoisomerase activity²¹.

Borromean rings are a set of linked circles that completely unlink upon the scission of any one of them. The use of a three-armed branched junction built from right-handed B-DNA and a three-armed branched junction built from left-handed Z-DNA allowed the production of three-ring Borromean rings²² (Fig. 3f). A single scission event can lead to the unlinking of all of the rings; in principle, this system can be extended to any number of rings.

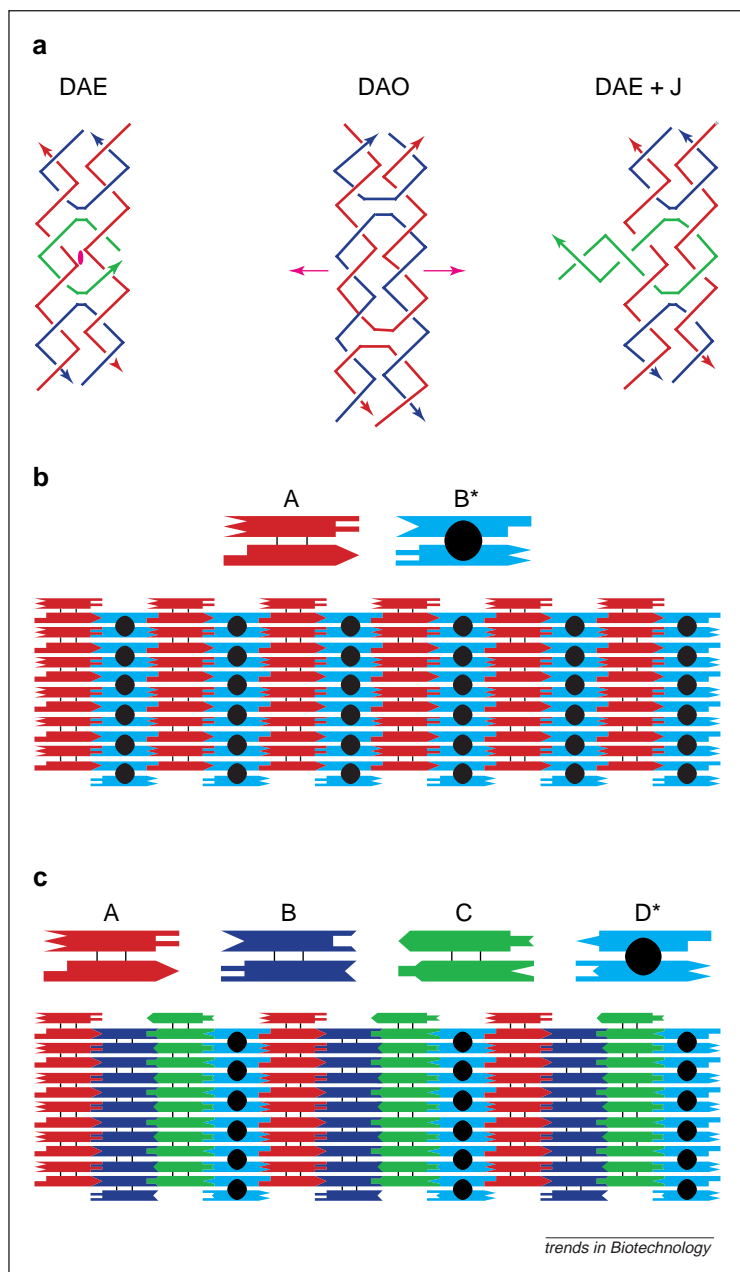


Figure 4

Double-crossover (DX) molecules and arrays assembled from them. **(a)** Two antiparallel DX isomers, known as DAE and DAO. The symmetry axis of DAE is normal to the page (symmetry is broken by the nick in the central strand) and that of DAO is horizontal within the page; in the case of DAO, strands of opposite color (red or blue) are related by symmetry. The third structure, DAE+J, is a DAE molecule in which an extra junction replaces the nick in DAE. **(b, c)** Two-dimensional patterned arrays derived from DX molecules. **(b)** The top of this panel shows two DX molecules with complementary sticky ends shown as complementary geometrical shapes. **A** is a conventional DX molecule, but **B*** is a DX+J molecule, in which a DNA hairpin protrudes from the plane defined by the helix axes of the two antiparallel domains. Shown below these molecules is an array of the two components fitting together to tile a plane. **(c)** A four-component array. The difference here is that the array has four components, where **A, B** and **C** are conventional DX molecules, and **D*** is a DX+J motif. It is clear from the bottom portion of the panel that the stripes should be separated by twice the distance seen in **(b)**.

Periodic arrays from DNA double-crossover molecules

To exploit the full power of this system, it is necessary to have rigid components. The DNA double-crossover

molecule (DX), a recombinational motif related to the Holliday junction, has this property²³. There are five different DX motifs, of which three contain parallel helical domains and two contain antiparallel domains²⁴. Parallel molecules are known to be meiotic intermediates²⁵ but they are not well behaved when the separation between their crossover points is short. By contrast, antiparallel DX molecules are well behaved. Two isomers of antiparallel DX molecules – DAO and DAE (Fig. 4a) – whose molecular topologies differ in having an odd (DAO) or even (DAE) number of double-helical half turns between crossover points. A third motif (Fig. 4a), DAE+J, consists of one or more bulged junctions positioned between the crossovers; the bulge consists of two nucleotides, whose presence enables the helix that is interrupted to be stacked. This extra helix can act as a topographic marker in the atomic-force microscope (AFM) when positioned so that it protrudes from the plane of the two DX helices.

These DX molecules can be used to ‘tile’ a plane (Fig. 4b). The molecules are about 16 × 4 nm and so the vertical repeat distance of the array in Fig. 4b is 4 nm and the horizontal repeat is 32 nm. The AFM cannot resolve distances as small as 4 nm, so the protruding features appear as stripes separated by 32 nm²⁶. The pattern can be controlled by using different components; using four components (Fig. 4c), for example, the spacing seen in the AFM is 64 nm²⁶. The features that produce the pattern consist of DNA, so it is also possible to change the pattern by using DNA-modification techniques. We have demonstrated that it is possible to modify these patterns by restriction, ligation and hybridization²⁷.

Periodic arrays from DNA parallelograms

The structure of the Holliday junction in solution^{28,29} is shown in Fig. 5a,b. The four arms visible in Fig. 1a stack in two adjacent pairs (arms I and II stack together, as do arms III and IV) to form two helical domains. Fig. 5a is a view down the dyad axis relating these domains and Fig. 5b shows a view at right angles to this, showing that there is an angle of about 60° between the helices. Although the individual junction is flexible, it is possible to produce a structure with adequate rigidity by combining four of them into a parallelogram-like structure³⁰ (Fig. 5c). This structure contains two parallel edges in one plane and the other pair of edges in a second plane about 2 nm behind it. Only the four crossover points are expected to be coplanar.

The helical domains illustrated in Fig. 5c each contain six double-helical turns, and the branch points are separated by four turns; there is a single helical turn between each crossover point and the boundary of the molecule. Attaching sticky ends to the tips of the helical domains enables these components to self-assemble into periodic arrays. The product of one-dimensional assembly (Fig. 5d) is a railroad-track structure containing helices at alternating distances of two and four helical turns (termed a 4+2 motif)³⁰. If all the helices contain complementary sticky ends on their opposite ends, the structure shown in Fig. 5e can self-assemble. This is a two-dimensional periodic array in which the 4+2 motif has been squared to produce cavities of dimension 4×4 and 2×2 helical turns, as well as two cavities 4×2 turns in size. Features corresponding to these spacings are prominent in AFM studies of this self-assembling array³⁰. It is

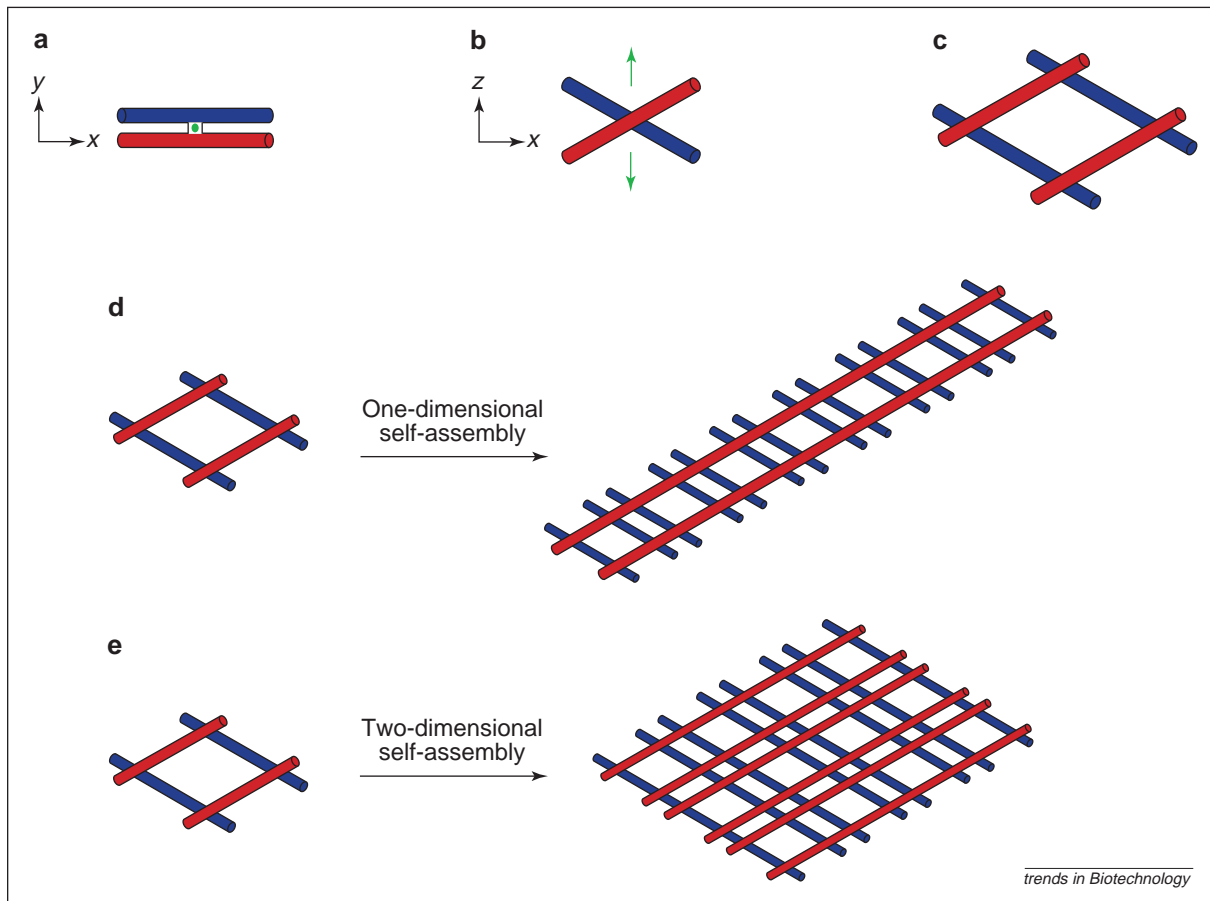


Figure 5

Parallelogram-like molecular components and their assembly. **(a)** A view down the dyad axis of the solution structure of a Holliday junction; the dyad axis is indicated by the small green dot. The blue helical domain is rotated 30° about the vertical so that its right end penetrates the page, and the red helical domain is rotated 30° about the vertical so that its left end penetrates the page. The x and y axes of a right-handed coordinate system are shown for orientation. **(b)** A view with the dyad axis vertical, the molecule having been rotated 90° about the x axis, as indicated by the coordinate axes. The dyad axis is indicated by the double arrows. **(c)** Combining four junctions in the same orientation as **(b)** into a parallelogram-like motif. There are six turns of DNA in each helix and four turns between crossover points, leading to a one-turn overhang on each end. **(d)** One-dimensional self-assembly of the motif into a railroad track-like array. The blue 'ties' are separated by alternating distances of four turns and two turns. **(e)** Two-dimensional self-assembly produces a lattice-work of DNA. The array shows the two-dimensional self-assembly product of the motif; the long separations between helices contain four helical turns and the short separations two turns. The lattice-work array contains two separate layers: an upper layer oriented from lower left to upper right and a lower layer oriented from lower right to upper left.

possible to 'tune' the sizes of the cavities; for example, we have made the product of a $4+2$ motif and a $6+2$ motif to produce an array whose parallelograms consist of 6×4 , 6×2 , 4×2 and 2×2 helical turns³⁰.

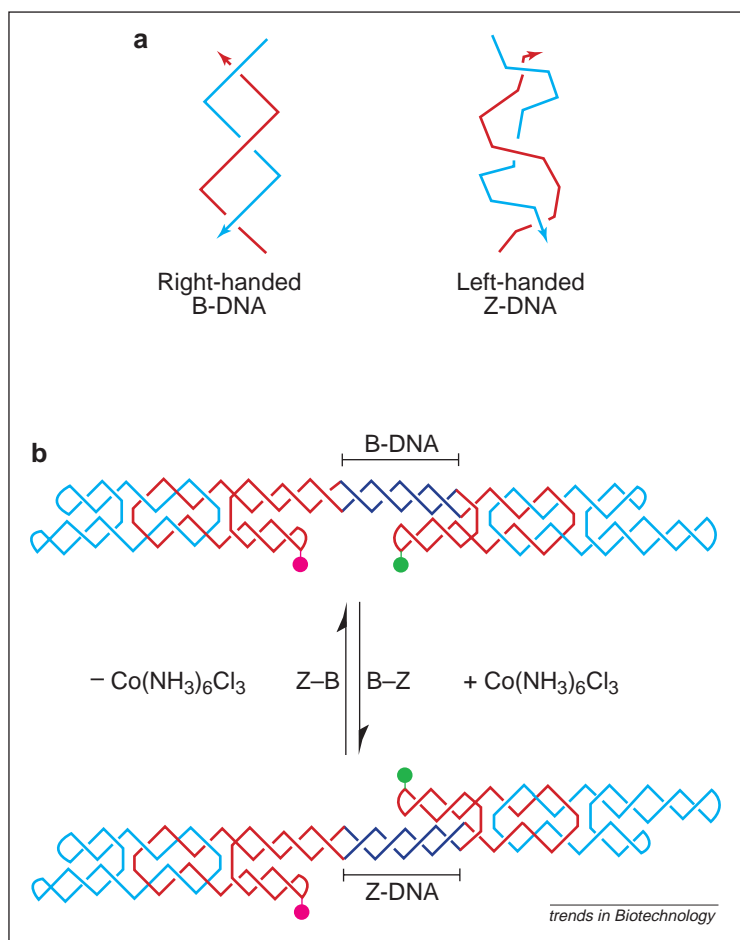
A nanomechanical DNA device

The structures and arrays described above are all static. However, we want to produce a nanomechanical device. The minimal mechanical device is a molecule whose structure switches between two alternatives in response to an external signal. We have developed a two-state device predicated on the B–Z transition of DNA. Conventional DNA, known as B-DNA, is a right-handed molecule. However, there is another structure of DNA that is radically different from B-DNA, known as Z-DNA¹⁹. Z-DNA is a left-handed molecule, but it is not the mirror image of B-DNA because it is also composed of sugars in the D configuration (Fig. 6a).

Two conditions must be met to obtain the Z-DNA structure: first, a sequence (called a proto-Z sequence)

that can be converted from B-DNA to Z-DNA; second, a solution environment that will promote the B–Z transition. The best known of the proto-Z sequences contains alternating C and G residues $[(dCdG)_n]$. High ionic strength and effectors such as $\text{Co}(\text{NH}_3)_6\text{Cl}_3$ can promote the B–Z transition¹⁹. The sequence requirement allows us to limit the B–Z transition in space, and the environmental requirement permits us to limit it in time.

To produce a two-state mechanical device, the two states must also be structurally well defined. Rigid components are needed for this, just as they are needed for periodic arrays. Consequently, the development of the device awaited the discovery that the DX molecule behaves as a rigid species. Once that was established²³, it was possible to design the molecular device illustrated in Fig. 6b, consisting of two DAO molecules connected by 4.5 turns of double-helical DNA. This connecting helix contains 20 bp of proto-Z DNA. In the absence of Z-promoting conditions, this segment will be in the right-handed B-form and the two unconnected


Figure 6

A DNA nanomechanical device. (a) The working portion of the device. The two forms of DNA in the device are shown in schematic fashion: right-handed B-DNA and left-handed Z-DNA. (b) The operation of the device. The device consists of two double-crossover DNA molecules (DAO motif) connected by 4.5 turns of DNA between the nearest crossover points. The upper portion illustrates the molecule constructed entirely from right-handed B-DNA. Three strands are shown: a red one in the center and two cyan strands on the ends triply catenated to it. Fluorescent dyes are drawn schematically as green (fluorescein) and magenta (Cy3) circles attached to the free hairpins near the middle of the molecule. At the center of the connecting helix is a 20-nucleotide region of proto-Z DNA in the B conformation (dark blue). When the B-Z transition is triggered by the addition of $\text{Co}(\text{NH}_3)_6\text{Cl}_3$, this same portion becomes left-handed Z-DNA, as seen at the bottom portion. When this transition occurs, the two double-crossover molecules change their relative positions, increasing the separation of the dyes. It is possible to cycle this system in both directions.

domains of the DAO components will be on the same side of the connecting helix. However, in Z-promoting conditions, the B-Z transition will occur and the two helices will be on opposite sides of the connecting helix.

The B-Z transition is largely a rotary motion, and so atoms on the bottom of the DAO motif on the right of the molecule will be displaced by a distance of 20–60 Å, depending on their distance from the axis of the connecting helix. Although shown as a half-turn rotation, the angular difference between the two states is about 3.5 turns. It is possible to monitor the state of the molecule by means of fluorescence-resonance-energy transfer. Energy transfer between the two fluorescent groups is a function of the inverse sixth power of their separation. The two groups are designed to be closer together in B-DNA than in Z-DNA, and

so the energy transfer is much higher when the device is in B-promoting conditions than when it is in Z-promoting conditions; a control molecule, lacking the proto-Z sequence, does not show this effect³¹.

Prospects for structural DNA nanotechnology

The experimental results described above augur well for the use of DNA self-assembly to produce structural targets on the nanometer scale. The resolution of control in this system is about an order of magnitude above the atomic scale; however, this is the scale on which the cell builds its structural components and it is likely to be appropriate for biological goals. During the next decade, it is reasonable to expect that periodic systems will be extended to three dimensions and that they will be combined with nanomechanical devices. The development of DNA-based scaffolding systems for non-biological applications such as molecular electronics may require the incorporation of new backbone molecules into this system; these would include uncharged backbones and other modifications directed more closely towards those applications.

Two-dimensional periodic patterns can already be produced using this approach. Wang tiles (tiles that associate on the basis of directed associations between their edges^{32,33}) are capable of emulating a Turing machine and sets of them can produce specific aperiodic patterns whose arrangement is algorithmic rather than simply periodic³³. Winfree has made the exciting suggestion that branched DNA molecules can be treated as Wang tiles³; if reduced to practice, this approach will have a major impact on both DNA-based computation and algorithmically designed scaffolded materials, whose properties we can only begin to imagine.

Acknowledgments

The author's work has been supported by the US National Institute of General Medical Sciences (grant GM-29554), the US Office of Naval Research (grant N00014-98-I-0093), DARPA/National Science Foundation (grant NSF-CCR-97-25021) and the Information Directorate of the Rome NY Air Force Research Laboratory (F30602-98-C-0148).

References

- Seeman, N. C. (1982) *J. Theor. Biol.* 99, 237–247
- Holliday, R. (1964) *Genet. Res.* 5, 282–304
- Winfree, E. (1995) in *DNA Based Computers* (Lipton, R. and Baum, E., eds), pp. 199–215, American Mathematical Society, Providence, RI, USA
- Cohen, S. N., Chang, A. C. Y., Boyer, H. W. and Helling, R. B. (1973) *Proc. Natl. Acad. Sci. U. S. A.* 70, 3240–3244
- Qiu, H., Dewan, J. C. and Seeman, N. C. (1997) *J. Mol. Biol.* 267, 881–898
- Whole issue (1998) *Trans. Am. Crystal. Assoc.* 33, 1–173
- Caruthers, M. H. (1985) *Science* 230, 281–285
- Seeman, N. C., Rosenberg, J. M. and Rich, A. (1976) *Proc. Natl. Acad. Sci. U. S. A.* 73, 804–808
- Hagerman, P. J. (1988) *Annu. Rev. Biophys. Biophys. Chem.* 17, 265–286
- Seeman, N. C. (1998) *Annu. Rev. Biophys. Biomol. Struct.* 27, 225–248
- Seeman, N. C. (1998) *Angew. Chemie, Int. Ed. Engl.* 37, 3220–3238
- Ma, R.-I., Kallenbach, N. R., Sheardy, R. D., Petrillo, M. L. and Seeman, N. C. (1986) *Nucleic Acids Res.* 14, 9745–9753
- Petrillo, M. L., Newton, C. J., Cunningham, R. P., Ma, R.-I., Kallenbach, N. R. and Seeman, N. C. (1988) *Biopolymers* 27, 1337–1352

- 14 Chen, J. and Seeman, N. C. (1991) *Nature* 350, 631–633
- 15 Zhang, Y. and Seeman, N. C. (1994) *J. Am. Chem. Soc.* 116, 1661–1669
- 16 Zhang, Y. and Seeman, N. C. (1992) *J. Am. Chem. Soc.* 114, 2656–2663
- 17 Seeman, N. C. (1992) *Mol. Eng.* 2, 297–307
- 18 Du, S. M. and Seeman, N. C. (1994) *Biopolymers* 34, 31–37
- 19 Rich, A., Nordheim, A. and Wang, A. H.-J. (1984) *Annu. Rev. Biochem.* 53, 791–846
- 20 Du, S. M., Stollar, B. D. and Seeman, N. C. (1995) *J. Am. Chem. Soc.* 117, 1194–1200
- 21 Wang, H., Di Gate, R. J. and Seeman, N. C. (1996) *Proc. Natl. Acad. Sci. U. S. A.* 93, 9477–9482
- 22 Mao, C., Sun, W. and Seeman, N. C. (1997) *Nature* 386, 137–138
- 23 Li, X., Yang, X., Qi, J. and Seeman, N. C. (1996) *J. Am. Chem. Soc.* 118, 6131–6140
- 24 Fu, T. J. and Seeman, N. C. (1993) *Biochemistry* 32, 3211–3220
- 25 Schwacha, A. and Kleckner, N. (1995) *Cell* 83, 783–791
- 26 Winfree, E., Liu, F., Wenzler, L. A. and Seeman, N. C. (1998) *Nature* 394, 539–544
- 27 Liu, F., Sha, R. and Seeman, N. C. (1999) *J. Am. Chem. Soc.* 121, 917–922
- 28 Lilley, D. M. J. and Clegg, R. M. (1993) *Annu. Rev. Biophys. Biomol. Struct.* 22, 299–328
- 29 Seeman, N. C. and Kallenbach, N. R. (1994) *Annu. Rev. Biophys. Biomol. Struct.* 23, 53–86
- 30 Mao, C., Sun, W. and Seeman, N. C. (1999) *J. Am. Chem. Soc.* 121, 5437–5443
- 31 Mao, C., Sun, W., Shen, Z. and Seeman, N. C. (1999) *Nature* 397, 144–146
- 32 Wang, H. (1963) in *Proceedings of the Symposium in the Mathematical Theory of Automata*, pp. 23–26, Polytechnic Press, New York, NY, USA
- 33 Grünbaum, B. and Shephard, G. C. (1987) in *Tilings and Patterns*, pp. 583–608, W. H. Freeman

Automation of functional assays by flow injection fluorescence microscopy

Louis D. Scampavia, Peter S. Hodder, Ilkka Lähdesmäki and Jaromir Ruzicka

Bead-injection spectroscopy is a novel technique that uses immobilized eukaryotic cells on microbeads as a renewable biosensor for fluorescence microscopy. The use of a flow injection instrument allows fast functional assays that generate full kinetic characterization of a drug. Because the cell population is automatically replaced for each assay, variability is minimized, thus allowing greater accuracy.

Increasingly, biological R&D is focusing on investigating real-time dynamic events with living cells, and fluorescence microscopy has become a standard tool in such studies. Numerous fluorescent probes are available^{1–7} that enable the detection of specific components of complex biological chemistries with excellent sensitivity and selectivity. However, real-time analyses using microscopy have been restricted by three critical factors: (1) precise microfluidic control of reagent addition and removal; (2) inconsistent or irreproducible cellular responses; and (3) automation of microscopy-based experimentation.

First, poor microfluidic control of solutions in the cellular milieu can negate or even corrupt much of the intricate kinetic information generated from a cellular response. Although a variety of perfusion chambers are currently employed in microscopy, some have poorly defined flow profiles that prevent the introduction and removal of reagents in a uniform, reproducible and timely manner. Given that most cell colonies grow in an irregular fashion, media flow around the cells is unique for each experimental set-up, despite the use of

a specific perfusion chamber. Moreover, standard kinetic models assume that perfusion generates an instantaneous equilibrium between a reagent (e.g. agonist) and the cellular milieu. However, this condition is frequently not achieved and a hysteresis between the perceived dosing and the biological response occurs owing to diffusion-limited instead of kinetics-limited control of the reagent.

Second, biological interactions are inconsistent owing to physiological stress and changes in the viability and variability of the cellular material. Poor flow-chamber design can induce a shear-stress response from the cells, and poor control of environmental factors at the microscope stage can also distress the cell population. Prolonged exposure to intense radiation [e.g. ultraviolet (UV) or infrared (IR) light] or cytotoxic reagents during an assay can irreversibly damage both the fluorescent probe (e.g. photobleaching) and the biological materials or cells. In both instances, this will limit the number of measurements possible on any selected colony of cells, making sequential stimulations unreliable or complicating data interpretation.

Finally, current advances in fluorescence microscopy have concentrated on the development of improved instrumentation, imaging and computational processing. Unfortunately, the automation of cell and solution handling has yet to be adequately addressed and still

L. D. Scampavia (scamp@u.washington.edu), P. S. Hodder, I. Lähdesmäki and J. Ruzicka (ruzicka@chem.washington.edu) are at the Department of Chemistry, University of Washington, Box 351700, Seattle, WA 98195-1700, USA.